Bond Strength of Lap-Spliced GFRP Bars in Concrete Beams

M. Reza Esfahani[1]; Mehrollah Rakhshanimehr[2]; and S. Roohollah Mousavi[3]

Abstract: In this paper, the bond strength of lap-spliced glass fiber–reinforced polymer (GFRP) bars in concrete beams is experimentally investigated. Thirteen beam specimens were manufactured for laboratory experiments. The parameter of transverse reinforcement along the splice length was selected as the main variable for the beam specimens. Other variables were surface properties of GFRP bars, bar diameter, and concrete compressive strength. Test results show that the effect of transverse reinforcement on bond strength between GFRP bars and concrete depends on the surface properties of reinforcing bars. The experimental results obtained in the present study and the results reported in the literature are compared with the current design equation provided by the American Concrete Institute (ACI) Committee 440 guidelines. The equation of ACI Committee 440 for evaluating the bond strength of GFRP bars underestimates the bond strength of spliced GFRP bars confined with large amounts of transverse reinforcement. For cases of small values of transverse reinforcement and splices without transverse reinforcement, the equation of ACI Committee 440 is unconservative and overestimates the bond strength. In this paper, an equation for predicting the bond strength of GFRP bars is also proposed on the basis of test results and the Monte Carlo simulation method. **DOI: 10.1061/(ASCE)CC.1943-5614.0000359.**

CE Database subject headings: Bonding; Fiber reinforced polymer; Concrete beams; Reinforced concrete; Transverse shear; Simulation.

Author keywords: Bond; Bar surface property; Glass fiber–reinforced polymers (GFRPs); Reinforced concrete beams; Splice length; Transverse reinforcement.

Introduction

Recently, fiber-reinforced polymer (FRP) bars have become an alternative to steel reinforcement for concrete structures in corrosive environments. Because FRP materials are nonmagnetic, they can be used when magnetic transparency is desirable [American Concrete Institute (ACI) Committee 440 2006].

Bond between FRP bars and concrete is a critical design parameter that controls the performance of reinforced concrete members. The bond strength of FRP bars and concrete depends on several factors, such as bar surface properties, bar diameter, concrete cover, development length, and amount of transverse reinforcement (Aly 2005; ACI Committee 440 2006).

The FRP reinforcing bars are produced with different types of surface properties, such as sand coated, spiral wrapped, helical/ribbed, and indented. The CAN/CSA S806 [Canadian Standard Association (CSA) 2002] code specifies different factors for different bar surface properties for evaluating the development length of FRP bars. However, Wambeke and Shield (2006) and Mosley et al. (2008) reported that the bar surface properties do not seem to affect the bond strength of FRP bars in concrete. Conversely, Banea et al. (2009) showed that bar surface properties have significant influences on bond strength.

Transverse reinforcement has an important role in the bond strength of spliced bars in beams. According to Darwin et al. (1996), transverse reinforcement in beams that had steel reinforcing bars with a high relative rib area had more beneficial increases in the bond force over same-sized steel bars with moderate rib area. There is a lack of data on the effect of transverse reinforcement on the bond behavior of FRP bars in concrete. Furthermore, there are contradictions between the results of previous studies regarding the effect of transverse reinforcement on the bond strength of FRP bars. In the Wambeke and Shield (2006) study, the database analysis showed that transverse reinforcement has no effect on the bond strength between FRP bars and concrete. According to ACI Committee 440 (2006), the glass fiber–reinforced polymer (GFRP) bars have a very low relative rib area, and thus the presence of transverse reinforcement may not increase the bond strength. In the ACI 440.1R-06 guidelines (ACI Committee 440 2006), the effect of transverse reinforcement on bond strength has been ignored. Aly (2005) has stated that transverse reinforcement increases the bond strength of splices. Harajli and Abouniaj (2010) have also shown that transverse reinforcement increases the bond strength of GFRP bars.

Limited tests have been conducted to study the bond strength of GFRP bars; most of them are beam-end and notched-beam tests. Therefore, it is important to develop test data for GFRP reinforcement on the basis of tests that provide more realistic measures of bond strength such that a reliable method can be developed for the splicing of GFRP reinforcement. In this paper, the results of an experimental study for evaluating the bond performance between GFRP bars and concrete in spliced bars are reported. The main

[1]Professor, Dept. of Civil Engineering, Ferdowsi Univ. of Mashhad, Mashhad, Iran. E-mail: esfahani@um.ac.ir

[2]Ph.D. Candidate in Structural Engineering, Dept. of Civil Engineering, Ferdowsi Univ. of Mashhad, Mashhad, Iran. E-mail: rakhsh_77@yahoo.com

[3]Assistant Professor, Dept. of Civil Engineering, Univ. of Sistan and Baluchestan, Zahedan, Iran (corresponding author). E-mail: se_mu15@stu-mail.um.ac.ir; s.r.mousavi@eng.usb.ac.ir

Note. This manuscript was submitted on March 9, 2012; approved on January 2, 2013; published online on January 4, 2013. Discussion period open until November 1, 2013; separate discussions must be submitted for individual papers. This paper is part of the ***Journal of Composites for Construction***, Vol. 17, No. 3, June 1, 2013. © ASCE, ISSN 1090-0268/2013/3-314-323/$25.00.

aim of this study is to explain the effect of specific bond parameters that are believed to be controversial. These parameters include the effect of transverse reinforcement and surface properties of GFRP bars on bond strength. Developing a new design equation using the test results and the Monte Carlo simulation method and assessing the accuracy of the ACI 440.1R-06 guidelines (ACI Committee 440 2006) for evaluating the bond strength of GFRP bars, in relation to the current test data, are additional aims of this investigation.

Design and Construction of Lap-Spliced RC Beam Specimens

Materials

The concrete mixtures were designed for an average target cylinder compressive strength of 40 [normal-strength concrete (NSC)] and 70 [high-strength concrete (HSC)] MPa after 28 days. Type I portland cement was used for all concrete mixtures. The maximum sizes of coarse aggregates were 25 and 12 mm for NSC and HSC, respectively. Silica fume and superplasticizer were used in the concrete mixture of the specimens made with 70-MPa HSC. From each concrete mixture, five 150×300 mm cylinders were cast for the determination of compressive strength. The proportions of concrete mixtures are summarized in Table 1.

The GFRP reinforcing bars were obtained from two different suppliers. The GFRP reinforcing bar properties reported by the manufacturer are summarized in Table 2. To evaluate the effect of bar surface properties, two types of bars—sand coated and ribbed—were used. The GFRP bars are shown in Fig. 1.

Test Specimens

Thirteen GFRP-reinforced concrete beam specimens with total span length of 2,300 mm and 2,000 mm center-to-center of roller supports, simply supported at the ends and with dimensions of 150×200 mm were cast and subjected to a four-point bending test. The constant moment region and shear span of beams were 600 and 700 mm, respectively. All of the beam specimens had two tensile GFRP bars spliced within the constant bending moment region. Conventional 6-mm-diameter steel stirrups spaced at 80 mm were used in the shear span. Two 6-mm-diameter steel bars were used as top reinforcement for supporting the stirrups.

Table 1. Mixture Proportions Used for Different Test Series

Mix series	NSC	HSC
Water/cement	0.40	0.28
Water (kg/m^3)	180	156
Cement (kg/m^3)	450	520
Coarse aggregate, 12–25 mm (kg/m^3)	600	—
Coarse aggregate, 6–12 mm (kg/m^3)	170	635
Fine aggregate, 0–6 mm (kg/m^3)	975	1,050
Silica fume (kg/m^3)	—	41.60
Superplasticizer (kg/m^3)	2.25	4.20

Table 2. Mechanical Properties of GFRP Bars

Groups	E_{frp}	f_u	Surface properties
I	>37	>700	Sand coated
II	>60	>1,000	Ribbed

Note: E_{frp} = modulus of elasticity of GFRP bars; f_u = ultimate tensile strength of GFRP bars.

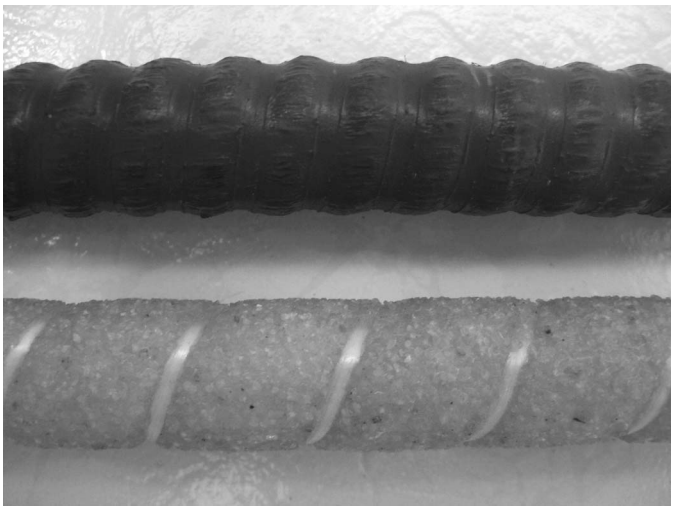

Fig. 1. GFRP reinforcement bars used in this study

The beam specimens were divided into two groups as shown in Table 3. In the first group, three specimens were longitudinally reinforced with two tensile 10-mm-diameter sand-coated GFRP bars. In this group, concrete with compressive strength of approximately 40 MPa was used. The main parameter investigated in this group was the amount of transverse reinforcement along the splice length. In Group I, one specimen did not have transverse reinforcement along its splice length, and two other specimens had transverse reinforcement with two different spacings of 20 and 80 mm. In the second group, three series of specimens were reinforced with ribbed GFRP bars. The main parameters investigated in these three series were the amount of transverse reinforcement along the splice length, bar diameter, and concrete compressive strength. In the first series, four specimens were longitudinally reinforced with 16-mm-diameter GFRP bars. In this series, one beam did not have transverse reinforcement along its splice length. Three other specimens had transverse reinforcement with three different spacings (50, 100, and 150 mm) along the splice length. Concrete with compressive strength of approximately 40 MPa was used for these specimens. In the second series, three specimens were reinforced with 12-mm-diameter GFRP bars, with three different spacings of transverse reinforcement—50, 100, and 150 mm—along the splice length. Concrete with compressive strength of approximately 40 MPa was also used for these specimens. The bar diameter in Series i and ii specimens was different to study the effect of bar diameter on bond strength. In the third series, three specimens were reinforced with 12-mm-diameter GFRP bars, with three different spacings of transverse reinforcement—50, 100, and 150 mm—along the splice length. Concrete with compressive strength of approximately 70 MPa was used for these specimens. Concrete strength in Series ii and iii was different to study the effect of concrete strength on bond strength. Dimensions and reinforcement details of the beam specimens and the position of the applied loads are shown in Fig. 2.

The specimens in Groups I and II had different splice lengths. The splice length of specimens in Group I was determined on the basis of ACI Committee 440 guidelines (2006). After the test of specimens in Group I with 180-mm splice length, it was observed that the splice failure of these specimens occurred in pullout mode. Thus, for the rest of the specimens in Group II, the splice length was increased to 400 mm for the possibility of having splitting type of bond failure.

J. Compos. Constr. 2013.17:314-323.

Table 3. Details of Beam Specimens

Groups	Series	Specimen	f'_c (MPa)	d_b (mm)	L_d (mm)	Stirrup diameter (mm)	S (mm)	C_x (mm)	C_y (mm)	C_s (mm)	C/d_b	L_d/d_b
I	—	S10-40-NC	39	10	180	8	—	30	30	50	3.0	18.0
		S10-40-S80					80	30	30	50	3.0	
		S10-40-S21					21	30	30	50	3.0	
II	i	R16-40-NC	41	16	400	8	—	30	25	25	1.3	25.0
		R16-40-S150					150	30	25	25	1.3	
		R16-40-S100					100	30	25	25	1.3	
		R16-40-S50					50	30	25	25	1.3	
	ii	R12-40-S150	41	12	400	8	150	43	25	15	1.1	33.3
		R12-40-S100					100	43	25	15	1.1	
		R12-40-S50					50	43	25	15	1.1	
	iii	R12-70-S150	72	12	400	8	150	43	25	15	1.1	33.3
		R12-70-S100					100	43	25	15	1.1	
		R12-70-S50					50	43	25	15	1.1	

Note: Specimen label: first letter = type of surface properties (R, ribbed; S, sand coated); first number = bar diameter (mm); second number = concrete compressive strength (MPa); second letter/third number = transverse reinforcement within splice length (S150, S100, S80, S50, and S21 are transverse reinforcement with spacings of 150, 100, 80, 50, and 21 mm); and NC indicates specimen without transverse reinforcement. Thus, for example, S10-40-S80 indicates that bar diameter is 10 mm with sand-coated surface, and concrete compressive strength is 40 MPa with transverse reinforcement spacing of 80 mm.

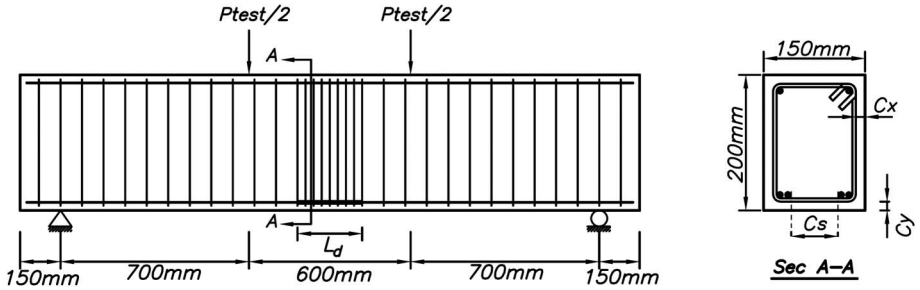

Fig. 2. Details of test specimens

Test Setup

Two concentrated loads were applied to the specimen by means of a hydraulic jack and a spreader beam (Fig. 3). A load cell was placed directly under the hydraulic jack and on the top of the spreader beam to transfer the load increments to a data logger acquisition system. A linear variable displacement transducer (LVDT) was placed at the center of the specimen to transfer the midspan displacements to the data logger. The load increments and the corresponding displacements were read directly on the data logger. The crack growth of the specimens during loading and at the time of failure was monitored.

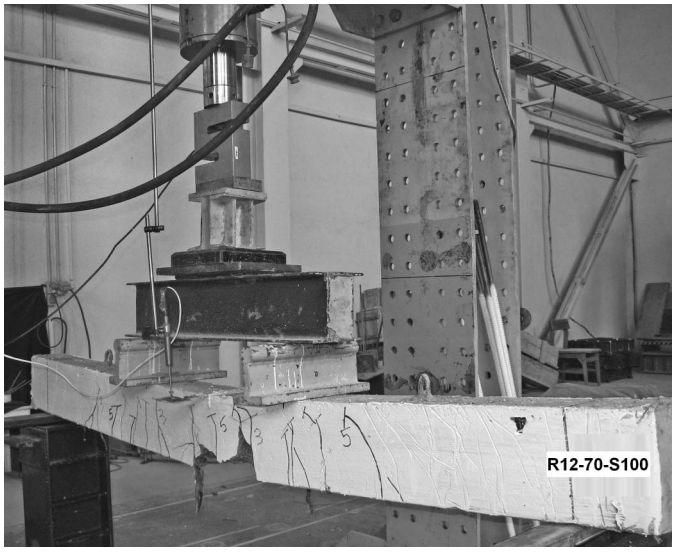

Fig. 3. Test setup

Experimental Results

Bond Strength of Specimens

The bond strength of the specimens of each group is presented in Table 4. The bond strength was determined by calculating the stress achieved in the reinforcement. The bar stress for all specimens was calculated from the measured maximum moment using elastoplastic analysis. This solution has been verified and used by different researchers (Tighiouart et al. 1999; Aly 2007; Mosley et al. 2008; Harajli and Abouniaj 2010). On the basis of the elastoplastic analysis, the tensile bar stress can be calculated by Eq. (1), as follows:

$$f_s = \frac{M_{\text{test}}}{A_f jd} \tag{1}$$

J. Compos. Constr. 2013.17:314-323.

Table 4. Test Results

Groups	Series	Specimen	P_{test} (kN)	M_{test} (kN • m)	u_{test} (MPa)	Failure mode
I	—	S10-40-NC	32.31	11.31	6.73	Splitting
		S10-40-S80	32.48	11.37	6.77	Pullout
		S10-40-S21	34.96	12.24	7.29	Pullout
II	i	R16-40-NC	37.59	13.16	2.18	Splitting
		R16-40-S150	55.26	19.34	3.20	Splitting
		R16-40-S100	72.18	25.26	4.18	Splitting
		R16-40-S50	89.47	31.31	5.18	Splitting
	ii	R12-40-S150	56.51	19.78	4.31	Splitting
		R12-40-S100	67.42	23.60	5.14	Splitting
		R12-40-S50	81.58	28.55	6.22	Splitting
	iii	R12-70-S150	54.88	19.21	4.19	Splitting
		R12-70-S100	67.41	23.60	5.14	Splitting
		R12-70-S50	86.97	30.44	6.64	Splitting

Note: P_{test} = maximum measured load at failure; M_{test} = maximum measured moment at failure; and u_{test} = experimental bond strength.

where M_{test} denotes maximum moment at failure and is equal to 0.7 $P_{test}/2$; A_f = cross-sectional area of all spliced tensile reinforcing bars (mm^2); and jd = resistant moment arm.

To calculate the average bond stress (u_{test}), the total force developed in the FRP reinforcement ($A_b \times f_s$) is divided by the contact area between the reinforcement and concrete in the splice length ($\pi \times d_b \times L_d$) as follows:

$$u_{test} = \frac{A_b f_s}{\pi d_b L_d} \tag{2}$$

where f_s = stress developed in reinforcement (MPa) as calculated by using Eq. (1); d_b = diameter of longitudinal reinforcement (mm); L_d = splice length (mm); and A_b = cross-sectional area of single spliced tensile reinforcing bar (mm^2).

Crack Growth and Failure of Specimens

Fig. 4 shows the crack growth and failure of different specimens. For a given series, each specimen started to crack at approximately the same loading level and had a flexural stiffness similar to other specimens before cracking. In general, the cracking initiated at the constant moment region of the specimens.

All lap-spliced specimens failed in bond along the splice length. The failure mode was splitting for all of the specimens reinforced with ribbed bars (Group II specimens). In specimens without transverse reinforcement and specimens with transverse reinforcement with spacings of 150 and 100 mm, failure occurred after longitudinal cracking in the splice region along the tensile reinforcement at the bottom and sides of the specimens. The cover in the splice region blew apart because of formation of longitudinal cracks on these surfaces (Fig. 4). With an increase in the amount of transverse reinforcement in Specimens R12-70-S50, R12-40-S50, and R16-40-S50, longitudinal cracks appeared only at the bottom of the beam. The presence of transverse reinforcement in the splice region of these specimens not only decreased the propagation of cracks, but also prevented the formation of longitudinal side cracks along the spliced bars. In these specimens, the concrete remained around the reinforcement after failure (Fig. 4).

The Specimen S10-40-NC, which was reinforced with sand-coated bars and did not have transverse reinforcement, failed in a splitting mode of failure. In contrast, Specimens S10-40-S80 and S10-40-S21 demonstrated a pullout mode of failure. These two specimens were similar to Specimen S10-40-NC except that they had transverse reinforcement in the splice region. In S10-40-S80 and S10-40-S21 specimens, a wide crack was formed at the splice ends (Fig. 4). It can be concluded that, for the specimens that were reinforced with sand-coated bars, the presence of transverse reinforcement in the splice region changed the failure mode from splitting to pullout. The lower value of $E_{frp}A_f$ for sand-coated GFRP bars compared with ribbed GFRP bars led to deeper cracks in specimens reinforced with sand-coated bars (Group I specimens).

Effect of Transverse Reinforcement

The bond strengths of R16-40-NC, R16-40-S150, R16-40-S100, and R16-40-S50 specimens (Series I of Group II specimens) are presented in Table 4. All of these specimens are reinforced with ribbed GFRP bars with a diameter of 16 mm and concrete with compressive strength of 41 MPa. The only variable in these specimens is the spacing of transverse reinforcement. Although the Specimen R16-40-NC does not have transverse reinforcement along the splice length, the spacing of transverse reinforcement in the other specimens varies from 50 to 150 mm. In Table 4, it is shown that the bond strength enhances with the increase of transverse reinforcement.

The effect of transverse reinforcement can be investigated by studying the bond strength of Specimens R12-40-S150, R12-40-S100, and R12-40S-50 in Series ii of Group II, and Specimens R12-70-S100, R12-70-S150, and R12-70-S50 in Series iii of Group II in Table 4. It is shown that by increasing the transverse reinforcement along the splice length, the bond strength of these specimens increases.

The effect of transverse reinforcement on spliced sand-coated bars can be evaluated by comparing the bond strength of Specimens S10-40-NC, S10-40-S80, and S10-40-S21 (Group I) in Table 4. It is shown that in specimens reinforced with sand-coated bars, transverse reinforcement does not have considerable effect on the bond strength of the spliced beam specimens.

Darwin et al. (1996) concluded that transverse reinforcement has more influence on the bond strength of spliced bars with a high relative rib area compared with those with moderate relative rib area. Therefore, the difference in the effect of transverse reinforcement on bond strength of ribbed and sand-coated bars might be related to the difference in their surface properties.

Effect of Concrete Compressive Strength

Based on their investigation, Tighiouart et al. (1998) concluded that the bond strength of GFRP bars to concrete does not increase with the concrete strength. The same results can be obtained from the tests of this study. The effect of concrete strength on bond strength of spliced bars can be investigated by comparing the test results of Series ii and iii of Group II specimens. The comparison of the test results in Table 4 shows that the concrete compressive strength does not influence the bond strength of GFRP bars in spliced beams considerably.

Effect of Bar Diameter

The effect of bar diameter on the bond strength of GFRP bars in concrete can be evaluated by comparing the bond strength of Series i and ii of Group II specimens (R16-40-S150, R12-40-S150; R16-40-S100, R12-40-S100; and R16-40-S50, R12-40-S50) in Table 4. The experimental results show that the bond strength of GFRP bars decreases with increase in the bar diameter. Tighiouart et al. (1998) and Hao et al. (2006) stated that when the diameter of

J. Compos. Constr. 2013.17:314-323.

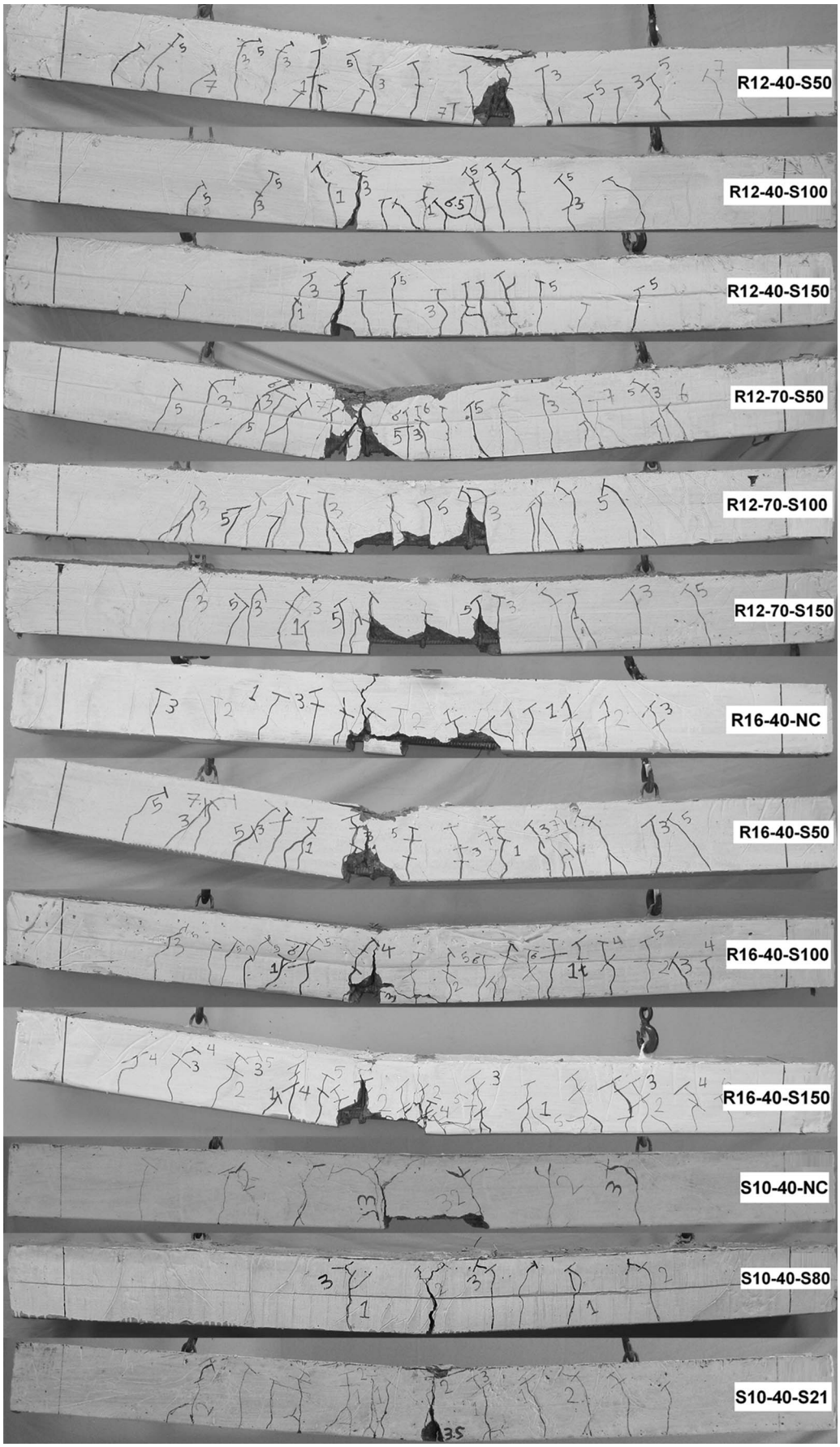

Fig. 4. Crack growth and failure state of test specimens

the bar is larger, more bleeding water is trapped beneath the bar. As a result, there is a greater possibility of creating voids around the bar, which will eventually decrease the contact surface between the concrete and the bar and thereby reduce the bond strength.

Comparison between Theoretical and Experimental Results

Specimens without Transverse Reinforcement

Wambeke and Shield (2006) used an approach similar to that used by Orangun et al. (1977) and proposed an equation for calculating the average bond strength of GFRP bars for splitting mode of bond failure as follows:

$$\frac{u}{0.083\sqrt{f'_c}} = \frac{1}{\alpha}\left(4.0 + 0.3\frac{C}{d_b} + 100\frac{d_b}{L_d}\right) \quad (3)$$

In its 2006 report, ACI Committee 440 endorsed the expression developed by Wambeke and Shield (2006) for calculating the bond strength of FRP bars (ACI Committee 440 2006). In Eq. (3), u is the bond strength between the FRP bar and concrete (in MPa); f'_c is the compressive strength of concrete (in MPa); C is the lesser of the cover to the center of the bar, or one-half of the center-to-center spacing of the bars being developed (in mm); d_b is the diameter of the bar (in mm); L_d is the embedment length of the reinforcement inside the concrete (in mm); and α is the factor of top bars effect. The ACI Committee 440 (2006) suggests the value of α to be taken equal to 1.5.

In Table 5, the bond strength of various beam specimens without transverse reinforcement is calculated in accordance with Eq. (3) and compared with the test results. Only the results of specimens with splitting mode of failure are taken into account. In Table 5, the trend of bond-strength predictions of Eq. (3) is generally consistent with the trend of test results. The predicted bond strengths are considerably larger than the test data, except for the Specimen S10-40-NC with small $L_d/d_b = 18$ and large $C/d_b = 3$, in which the ratio of test to predicted value is 1.23. If the result of the Specimen S10-40-NC is eliminated, the average ratio of test to predicted bond strength is 0.70 with a standard deviation of 0.10. Therefore, it can be concluded that Eq. (3) considerably overestimates the bond strength of spliced GFRP bars without transverse reinforcement along the splice length. In other words, the bond failure is highly probable if Eq. (3) is used for design of these types of beams. The majority of test results being considered for deriving Eq. (3) comprised the results of beam-end tests and notched-beam tests (Wambeke and Shield 2006).

Specimens with Transverse Reinforcement

For the specimens with transverse reinforcement, a comparison between the results of nine test specimens in this study and 22 other specimens from the literature (Tighiouart et al. 1999; Aly 2005; Harajli and Abouniaj 2010) with Eq. (3) is presented in Table 6. Only the results of specimens with splitting mode of failure are used. As shown in Table 6, the trend of bond-strength predictions of Eq. (3) for specimens reinforced with bars with low relative rib area (specimens with sand-coated, helical-wrapped, and grooved bars) is generally consistent with the trend of test results. The mean value of test to predicted bond-strength ratios for specimens reinforced with sand-coated bars is 0.79 with a standard deviation of 0.07; for specimens reinforced with helical-wrapped bars, the mean value is 0.81 with a standard deviation of 0.10. In one specimen

Table 5. Comparison between Proposed Equation and Eq. (3) with Test Results (Specimens without Transverse Reinforcement)

Reference	Beam number	Surface properties[a]	Failure mode	C/d_b	L_d/d_b	u_{test}	u_{test}/u Eq. (3)	u_{test}/u Eq. (5)
Mosley et al. (2008)	B-G1-3	W-SC	Splitting	2.9	19.0	2.95	0.82	1.21
	B-G2-3	Ribbed	Splitting	2.9	19.0	2.79	0.78	1.14
	B-A-3	Ribbed	Splitting	2.9	19.0	3.10	0.88	1.29
	B-A-1	Ribbed	Splitting	1.3	28.6	2.42	0.89	1.30
	B-A-2	Ribbed	Splitting	1.3	19.0	1.86	0.65	0.96
	B-G1-1	W-SC	Splitting	1.3	28.6	2.29	0.85	1.24
	B-G2-1	Ribbed	Splitting	1.3	28.6	1.94	0.73	1.06
	B-G1-2	W-SC	Splitting	1.3	19.0	1.73	0.60	0.88
	B-G2-2	Ribbed	Splitting	1.3	19.0	1.77	0.64	0.94
	Mean		—	—	—	—	0.76	1.11
	Standard deviation		—	—	—	—	0.11	0.16
Harajli and Abouniaj (2010)	R1.25-L15	Grooved	Splitting	1.8	15	3.53	0.55	0.93
	R1.25-L20	Grooved	Splitting	1.8	20	3.19	0.58	0.99
	R2-L15	Grooved	Splitting	2.6	15	3.60	0.55	0.93
	R2-L20	Grooved	Splitting	2.6	20	3.67	0.65	1.11
	R1.25-L30	Grooved	Splitting	1.8	30	2.24	0.48	0.81
	Mean		—	—	—	—	0.56	0.95
	Standard deviation		—	—	—	—	0.06	0.11
Aly (2005)	G70z-A23	SC	Splitting	2.6	36.7	2.54	0.62	1.05
	G70z-A22	SC	Splitting	2.6	36.7	2.40	0.58	0.97
	Mean		—	—	—	—	0.60	1.01
	Standard deviation		—	—	—	—	0.03	0.06
Current study	R16-40-NC	Ribbed	Splitting	1.3	25.0	2.18	0.49	0.83
	S10-40-NC	SC	Splitting	3.0	18.0	6.73	1.23	—
All	Mean		—	—	—	—	0.70	1.05
	Standard deviation		—	—	—	—	0.10	0.15

[a]W-SC = wrapped–sand coated; SC = sand coated.

J. Compos. Constr. 2013.17:314-323.

Table 6. Comparison between Proposed Equation and Eq. (3) with Test Results (Specimens with Transverse Reinforcement)

Reference	Beam number	Surface properties[a]	Failure mode	C/d_b	L_d/d_b	u_{test}	u_{test}/u Eq. (3)	u_{test}/u Eq. (8)
Aly (2005)	G50N-A8	SC	Splitting	2.6	26.2	3.60	0.79	1.13
	G70N-A9	SC	Splitting	2.6	36.65	3.28	0.80	1.12
	G80N-A10	SC	Splitting	2.6	41.9	3.30	0.87	1.20
	G110N-A11	SC	Splitting	2.6	57.6	2.56	0.74	1.01
	G70L-A25	SC	Splitting	2.6	36.7	2.95	0.72	1.11
	G70N-A26	SC	Splitting	2.6	36.7	3.28	0.80	1.12
	G70M-A27	SC	Splitting	2.6	36.7	3.79	0.91	0.94
	G70N-KW28	SC	Splitting	1.8	36.7	2.83	0.70	0.97
	G70N-FX29	SC	Splitting	1.8	36.7	3.18	0.81	1.12
	G70N-KX30	SC	Splitting	2.6	36.7	3.28	0.80	1.12
	G70N-PX31	SC	Splitting	2.7	36.7	2.91	0.70	0.97
	G70N-KY32	SC	Splitting	2.6	36.7	3.61	0.89	1.24
	G70N-KY33	SC	Splitting	2.7	36.7	3.22	0.77	1.08
	Mean		—	—	—	—	0.79	1.09
	Standard deviation		—	—	—	—	0.07	0.09
Tighiouart et al. (1999)	A460-1	HW	Splitting	2.4	54.7	3.73	0.91	1.28
	A460-2	HW	Splitting	2.4	54.7	3.83	0.94	1.31
	A540-1	HW	Splitting	2.9	36.2	2.52	0.65	0.90
	A540-2	HW	Splitting	2.9	36.2	3.35	0.87	1.20
	B-675-1	HW	Splitting	2.9	42.5	3.11	0.82	1.17
	B-675-2	HW	Splitting	2.9	42.5	3.14	0.82	1.18
	B-870-1	HW	Splitting	2.4	42.5	2.44	0.69	0.98
	B-870-2	HW	Splitting	2.4	42.5	2.64	0.75	1.06
	Mean		—	—	—	—	0.81	1.14
	Standard deviation		—	—	—	—	0.10	0.14
Harajili and Abouniaj (2010)	R1.25L20-C	Grooved	Splitting	1.8	20	4.18	0.74	1.01
Current study	R16-40-S150	Ribbed	Splitting	1.3	25.0	3.20	0.72	0.95
	R16-40-S100	Ribbed	Splitting	1.3	25.0	4.18	0.94	1.12
	R16-40-S50	Ribbed	Splitting	1.3	25.0	5.18	1.16	1.07
	R12-40-S150	Ribbed	Splitting	1.3	25.0	4.31	1.11	1.31
	R12-40-S100	Ribbed	Splitting	1.1	33.3	5.14	1.32	1.36
	R12-40-S50	Ribbed	Splitting	1.1	33.3	6.22	1.60	1.19
	R12-70-S150	Ribbed	Splitting	1.1	33.3	4.19	0.81	0.97
	R12-70-S100	Ribbed	Splitting	1.1	33.3	5.14	1.00	1.03
	R12-70-S50	Ribbed	Splitting	1.1	33.3	6.64	1.29	0.96
	Mean		—	—	—	—	1.10	1.11
	Standard deviation		—	—	—	—	0.27	0.15
All	Mean		—	—	—	—	0.88	1.10
	Standard deviation		—	—	—	—	0.21	0.12

[a]SC = sand coated; HW = helical wrapped.

with grooved bars, the ratio of test to predicted bond strength is 0.74. Therefore, it can be concluded that Eq. (3) in specimens with transverse reinforcement considerably overestimates the bond strength of spliced GFRP bars with low relative rib area.

In the specimens with high relative rib area (specimens with ribbed bars in the current study), Eq. (3) underestimates the bond strength of spliced bars confined with larger values of transverse reinforcement along the splice length. The ratios of test to predicted value decrease as the amount of transverse reinforcement decreases.

There are some problems regarding the ACI Committee 440 (2006) guidelines [which are based on Eq. (3)] that are still controversial and therefore require further investigation (Harajli and Abouniaj 2010). The ACI Committee 440 (2006) guidelines do not account for the effects of surface properties of FRP bars and the amount of transverse reinforcement in bond-strength calculation. According to Harajli and Abouniaj (2010), the ACI Committee 440 (2006) guidelines for evaluating the bond strength of FRP bars should be based on a more rational approach in which commercially available FRP bars are classified depending on their surface deformation, rather than adoption of one common expression for all types of FRP bars.

Proposed Equation for Bond-Strength Calculation

Specimens without Transverse Reinforcement

To reduce the probability of bond failure, the right-hand side of Eq. (3) should be multiplied by a strength-reduction factor φ_b as follows:

$$\frac{u}{0.083\sqrt{f'_c}} = \varphi_b \frac{1}{\alpha}\left(4.0 + 0.3\frac{C}{d_b} + 100\frac{d_b}{L_d}\right) \quad (4)$$

The Monte Carlo simulation is used to obtain the value of φ_b. The average and the standard deviation values of f'_c and C are obtained by the method proposed by Darwin et al. (1998), whereas the

average and the standard deviation values of d_b and L_d are calculated by the method proposed by He and Tian (2011). A normal distribution is assumed for the previously mentioned random variables (Darwin et al. 1998; He and Tian 2011).

The results of test specimens without transverse reinforcement (Table 5) are used to determine the value of φ_b so that the probability of a test over predicted bond-strength ratio less than 1.0 is 22% (ACI Committee 440 2006). As mentioned previously, only results of specimens with splitting mode of failure are used in Table 5, and the Specimen S10-40-NC with $L_d/d_b = 18$ and $C/d_b = 3$ is ignored in the analysis. The elimination of this specimen does not hurt the overall evaluation because members with such low L_d/d_b and high C/d_b are not used in practice. The failure mode, the surface properties of the reinforcing bars, and the ratios of C/d_b and L_d/d_b of these specimens are shown in Table 5.

For each of the 17 specimens without transverse reinforcement, 1,000 Monte Carlo simulations are carried out. Using the results of these simulations, the value of φ_b is calculated to be 0.59. Multiplying Eq. (4) by this factor leads to

$$\frac{u}{0.083\sqrt{f'_c}} = \frac{1}{\alpha}\left(2.36 + 0.177\frac{C}{d_b} + 59\frac{d_b}{L_d}\right) \tag{5}$$

As proposed by CAN/CSA S806 (CSA 2002) and Esfahani et al. (2005), a top bar factor equal to 1.3 is used for top cast bars. Using Eq. (5), the mean value of test over predicted bond-strength ratios is 1.05 with a standard deviation of 0.15 (Table 5).

Specimens with Transverse Reinforcement

In this study, an approach similar to that used by Orangun et al. (1977) has been utilized to include the effect of transverse reinforcement. Orangun et al. (1977) showed that the bond strength of steel-reinforced spliced beam specimens with transverse reinforcement in the splice region can be given by

$$u/\sqrt{f'_c} = u_c/\sqrt{f'_c} + u_{tr}/\sqrt{f'_c} \tag{6}$$

where u_c = bond strength of spliced bars without transverse reinforcement; and u_{tr} = portion of bond strength contributed by transverse reinforcement.

Orangun et al. (1977) showed that the parameter representing the effect of transverse reinforcement is a function of the transverse bar's cross-section (A_{tr}), the transverse bar's yield stress (f_{yt}), the spacing between the transverse reinforcements along the splice length (S), and the diameter of the tensile reinforcement (d_b), as follows:

$$u_{tr}/\sqrt{f'_c} = f_R\frac{A_{tr}f_{yt}}{Sd_b} \tag{7}$$

Aly (2005) demonstrated that this equation is also valid for FRP reinforcements. Introducing Eqs. (7) and (5) into Eq. (6) leads to

$$u/\sqrt{f'_c} = \frac{1}{\alpha}\left[0.083\left(2.36 + 0.177\frac{C}{d_b} + 59\frac{d_b}{L_d} + f_R\frac{A_{tr}f_{yt}}{Sd_b}\right)\right] \tag{8}$$

Similar to the previous section, the Monte Carlo simulation method is used to obtain the coefficient f_R. For this purpose, the results of the test specimens with transverse reinforcement (Table 6) are used. Only the results of specimens with splitting mode of failure are used in Table 6. The results of two specimens in the current study (S10-40-S80 and S10-40-S21) and six specimens in the Harajli and Abouniaj (2010) study with pullout mode of failure are not used in obtaining the proposed equation. Also, there are a few specimens with unnecessarily long splice length $L_d/d_b > 78$ in the study conducted by Tighiouart et al. (1999). These specimens are ignored in this study. The elimination of these specimens does not hurt the overall evaluation because members with such high values of L_d/d_b are not used in practice. The failure mode, the surface properties of the reinforcing bars, and the ratios of C/d_b and L_d/d_b of the specimens are shown in Table 6.

Table 7. Numerical Values of f_R Factor

Surface properties	f_R
Helical wrapped	0.03
Grooved	0.08
Sand coated	0.17
Ribbed	0.21

Using the Monte Carlo simulation, a total of 1,000 simulated specimens are created for each of the 31 specimens presented in Table 6. A normal distribution is assumed for the random parameters E_s, A_{tr}, E_{frp}, and S. The average value and the standard deviation of E_s are obtained from the Val and Chernin (2009) study, A_{tr} from Lee et al. (2002), and E_{frp} and S from Darwin et al. (1998). In addition, a lognormal distribution is assumed for f_{yt} (Val and Chernin 2009; Lee et al. 2002). The average value and the standard deviation of f_{yt} are obtained from Val and Chernin (2009). The Monte Carlo simulations are used to determine the value of f_R so that the probability of a test over predicted bond-strength ratio less than 1.0 is 22% (ACI Committee 440 2006). The values of f_R for different bar surface properties are presented in Table 7. The surface properties of GFRP bars used in different test specimens are shown in Fig. 5. The mean of the test over predicted bond-strength ratios using Eq. (8) is 1.10 with a standard deviation of 0.12 (Table 6).

Further experimental studies are recommended to check the validity of the proposed equations. The authors are making initial

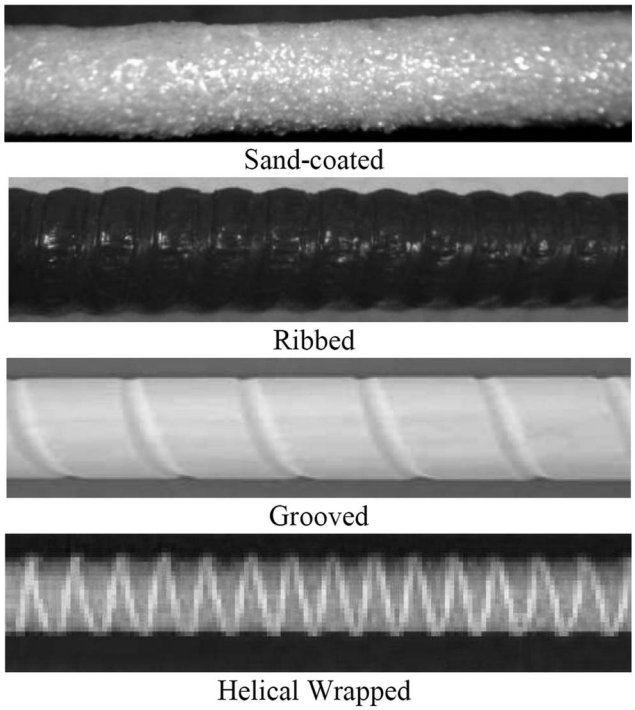

Fig. 5. Surface properties of reinforcement bars

J. Compos. Constr. 2013.17:314-323.

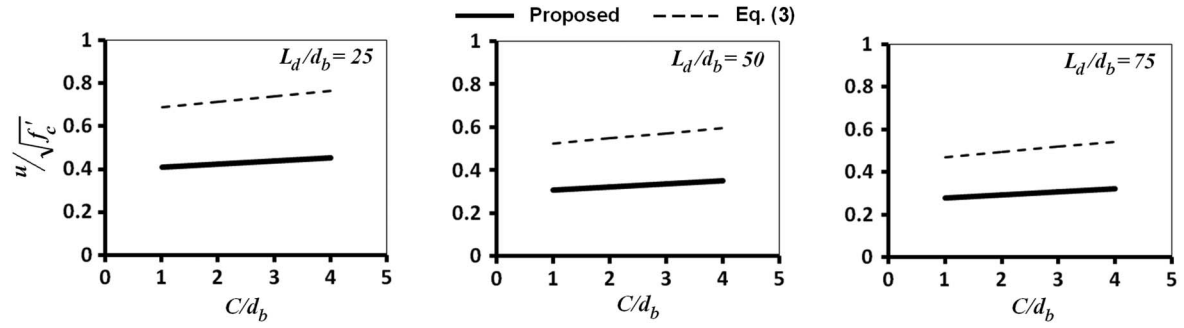

Fig. 6. Bond-strength comparison between proposed equation and Eq. (3) (specimens without transverse reinforcement)

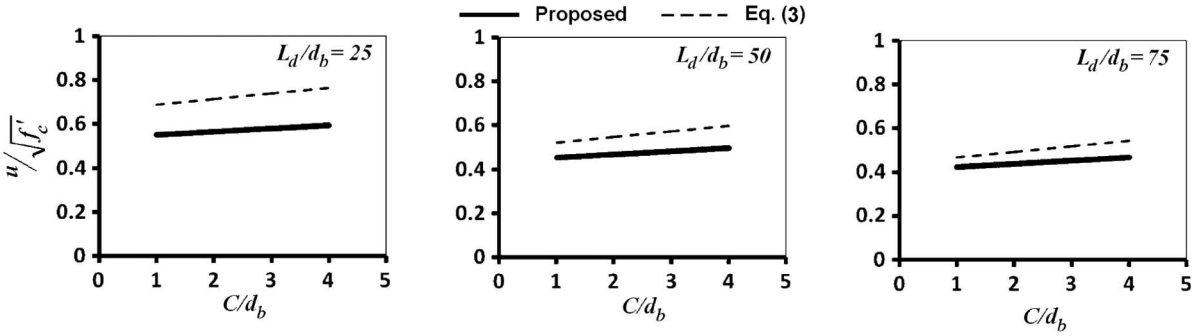

Fig. 7. Bond-strength comparison between proposed equation and Eq. (3) for ribbed bars (specimens with transverse reinforcement)

assessment of the modified equations, and more experimental results are needed for further verification. However, a parametric comparison between the proposed equations with Eq. (3) is provided in the next section.

Evaluation of Proposed Equations

The bond strengths calculated by the proposed equation and Eq. (3) are compared in Fig. 6 for specimens without transverse reinforcement and three different splice lengths of 25, 50, and 75 d_b. For all splice-length values, the bond strength calculated by the proposed equation is lower than that predicted by Eq. (3).

A parametric comparison between the proposed equation with Eq. (3) for specimens with transverse reinforcement and ribbed bars is provided in Fig. 7. The bond strengths calculated by the proposed equation and Eq. (3) are compared in Fig. 7 for three different splice lengths of 25, 50, and 75 d_b. The longitudinal bar diameter, transverse reinforcing bar diameter, and the spacing of transverse reinforcement are assumed to be 12, 8, and 150 mm, respectively. For all splice-length values, the bond strength calculated by the proposed equation is lower than that predicted by Eq. (3). The difference of bond-strength values between the proposed equation and Eq. (3) increases as the f_R factor decreases.

Conclusion

Based on the results of this study, the following conclusions are drawn:

1. All beam specimens reinforced with ribbed GFRP bars showed splitting mode of bond failure, whereas two specimens reinforced with sand-coated bars failed in pullout mode. Transverse reinforcement in specimens reinforced with sand-coated GFRP bars altered the bond failure mode from splitting to pullout.
2. The experimental results show that concrete compressive strength does not significantly influence the bond strength of GFRP bars in spliced beams. The bond strength of GFRP bars decreases with increase in the bar diameter.
3. In the case of ribbed GFRP bars, transverse reinforcement increases the bond strength of spliced bars. However, it does not have considerable effect on the bond strength of spliced sand-coated GFRP bars.
4. The guidelines of ACI Committee 440 for evaluating the bond strength of GFRP bars (ACI Committee 440 2006) overestimate the bond strength of spliced GFRP bars without transverse reinforcement. In these specimens, the average and standard deviation of test to predicted bond-strength ratios are 0.70 and 0.10, respectively.
5. The guidelines of ACI Committee 440 for evaluating the bond strength of GFRP bars (ACI Committee 440 2006) overestimate the bond strength of spliced GFRP bars with low relative rib area and confined with transverse reinforcement. The mean value of test to predicted bond-strength ratios for specimens reinforced with sand-coated bars is 0.79 with a standard deviation of 0.07; for specimens reinforced with helical-wrapped bars, the mean value is 0.81 with standard deviation of 0.10. In one specimen with grooved bars, the ratio of test to predicted bond strength is 0.74. In the specimens with high relative rib area (specimens with ribbed bars in the current study), Eq. (3) underestimates the bond strength of spliced bars confined with larger values of transverse reinforcement along the splice length. The ratio of test to predicted value decreases as the amount of transverse reinforcement decreases.
6. The equation proposed in the current study, based on the Monte Carlo simulation method for specimens failed by splitting mode, can be used to predict the bond strength of GFRP

J. Compos. Constr. 2013.17:314-323.

bars in specimens with and without transverse reinforcement along the splice length. The mean value of test over predicted bond-strength ratios is 1.05 with a standard deviation of 0.15 for specimens without transverse reinforcement, and 1.10 with a standard deviation of 0.12 for specimens with transverse reinforcement.

Notation

The following symbols are used in this paper:

A_b = cross-sectional area of single spliced tensile reinforcing bar;
A_f = cross-sectional area of all spliced tensile reinforcing bars;
A_{tr} = area of transverse reinforcement;
C = lesser of cover to center of bar or one-half of center-to-center spacing of bars being developed;
C_s = spacing between spliced bars;
C_x = side cover;
C_y = bottom cover;
d_b = diameter of longitudinal reinforcement;
E_{frp} = modulus of elasticity of FRP bars;
f_R = factor to include effect of surface properties on bond strength;
f_s = stress developed in reinforcement;
f_u = ultimate tensile strength of FRP bars;
f_{yt} = yield strength of transverse reinforcement;
f'_c = compressive strength of concrete;
jd = resistant moment arm;
L_d = splice length of reinforcement;
M_{test} = maximum measured moment at failure;
P_{test} = maximum measured load at failure;
S = spacing of transverse reinforcement;
u = calculated bond strength;
u_c = bond strength of spliced bars without transverse reinforcement;
u_{test} = experimental bond strength;
u_{tr} = portion of bond strength contributed by transverse reinforcement; and
α = top bar effect.

References

Aly, R. (2007). "Stress along tensile lap-spliced fiber reinforced polymer reinforcing bars in concrete." *Can. J. Civ. Eng.*, 34(9), 1149–1158.

Aly, R. S. M. (2005). "Experimental and analytical studies on bond behavior of tensile lap spliced FRP reinforcing bars in concrete." Ph.D. thesis, Univ. of Sherbrooke, Sherbrooke, Quebec, QC.

American Concrete Institute (ACI) Committee 440. (2006). "Guide for the design and construction of structural concrete reinforced with FRP bars." *ACI 440.1R-06*, Farmington Hills, MI.

Banea, M., Torres, L., Turon, A., and Barris, C. (2009). "Experimental study of bond behavior between concrete and FRP bars using a pull-out test." *Composites, Part B*, 40(8), 784–797.

Canadian Standard Association (CSA). (2002). "Design and construction of building components with fiber reinforced polymer." *CAN/CSA S806-02*, Rexdale, ON.

Darwin, D., Idun, E. K., Zou, J., and Tholen, M. L. (1998). "Reliability based strength reduction factor for bond." *ACI Struct. J.*, 95(4), 434–443.

Darwin, D., Zou, J., Tholen, M., and Idun, E. (1996). "Development length criteria for conventional and high relative rib area reinforcing bars." *ACI Struct. J.*, 93(3), 347–359.

Esfahani, M. R., Kianoush, M. R., and Lachemi, M. (2005). "Bond strength of glass fiber reinforced polymer reinforcing bars in normal and self consolidating concrete." *Can. J. Civ. Eng.*, 32, 553–560.

Hao, Q. D., Wang, B., and Ou, J. P. (2006). "Fibre reinforced polymer rebar's application to civil engineering." *Concrete*, 9, 38–40.

Harajli, M., and Abouniaj, M. (2010). "Bond performance of GFRP bars in tension: experimental evaluation and assessment of ACI 440 guidelines." *J. Compos. Constr.*, 14(6), 659–668.

He, Z., and Tian, G. (2011). "Reliability based bond design for GFRP-reinforced concrete." *Mater. Struct.*, 44(8), 1477–1489.

Lee, J. O., Yang, Y. S., and Ruy, W. S. (2002). "A comparative study on reliability index and target performance based probabilistic structural design optimization." *Comp. Struct.*, 80(3–4), 257–269.

Mosley, C. P., Tureyen, A. K., and Frosch, R. J. (2008). "Bond strength of nonmetallic reinforcing bars." *ACI Struct. J.*, 105(5), 634–642.

Orangun, C. O., Jirsa, J. O., and Breen, J. E. (1977). "Reevaluation of test data on development length and splices." *Proc. Am. Concr. Inst.*, 74(3), 114–122.

Tighiouart, B., Benmokrane, B., and Gao, D. (1998). "Investigation of bond in concrete member with fibre reinforced polymer (FRP) bars." *Constr. Build. Mater.*, 12(8), 453–462.

Tighiouart, B., Benmokrane, B., and Mukhopadhyaya, P. (1999). "Bond strength of glass FRP rebar splices in beams under static loading." *Constr. Build. Mater.*, 13(7), 383–392.

Val, D. V., and Chernin, L. (2009). "Serviceability reliability of reinforced concrete beams with corroded reinforcement." *J. Struct. Eng.*, 135(8), 896–905.

Wambeke, B., and Shield, C. (2006). "Development length of glass fiber reinforced polymer bars in concrete." *ACI Struct. J.*, 103(1), 11–17.

J. Compos. Constr. 2013.17:314-323.